Scenarios for the LHC Upgrade

W. Scandale, F. Zimmermann, CERN, Geneva, Switzerland

Abstract

The projected lifetime of the LHC low-beta quadrupoles, the evolution of the statistical error halving time, and the physics potential all call for an LHC luminosity upgrade by the middle of the coming decade. In the framework of the CARE-HHH network three principal scenarios have been developed for increasing the LHC peak luminosity by more than a factor of 10, to values above 10^{35} cm^{-2}s^{-1}. All scenarios imply a rebuilding of the high-luminosity interaction regions (IRs) in combination with a consistent change of beam parameters. However, their respective features, bunch structures, IR layouts, merits and challenges, and luminosity variation with β^* differ substantially. In all scenarios luminosity leveling during a store would be advantageous for the physics experiments. An injector upgrade must complement the upgrade measures in the LHC proper in order to provide the beam intensity and brightness needed as well as to reduce the LHC turnaround time for higher integrated luminosity.

1 MOTIVATION AND TIME FRAME

The Large Hadron Collider (LHC) will collide two proton beams with a centre-of-mass energy of 14 TeV at design and "ultimate" luminosities of 10^{34} cm^{-2}s^{-1} and 2.3×10^{34} cm^{-2}s^{-1}. The LHC proton beams will cross each other at the four detectors of the two high-luminosity experiments ATLAS and CMS, the B physics experiment LHCb, and the ion experiment ALICE. The LHC is set to explore an extremely rich physics landscape, spanning from the Higgs particle, over supersymmetry, extra dimensions, black holes, precision measurements of the top quark, the unitarity triangle, to the quark-gluon plasma [1].

Simple models for the LHC luminosity evolution over the first few years of operation [2] indicate that the IR quadrupoles may not survive for more than 8 years due to high radiation doses, and that already after 4–5 years of operation the halving time of the statistical error may exceed 5 years. Either consideration points out the need for an LHC luminosity upgrade around 2016. Actually there exists even a third reason for an LHC upgrade, which is extending the physics potential of the LHC: A ten-fold increase in the luminosity will increase the discovery range for new particles by about 25% in mass [1]. Detailed physics examples can be found in Ref. [3]. The particle-physicists' goal for the upgrade is to collect 3000 fb^{-1} per experiment in 3–4 years of data taking. Simlar upgrades were performed at previous hadron colliders, where, for example, the Tevatron upgrade has resulted in an integrated Run-II luminosity about 50 times larger than that of Run I.

The LHC upgrade could consist of a series of improvements, e.g. two stages – the first one consolidating the nominal performance and providing a luminosity of up to 3×10^{34} cm^{-2}s^{-1} and the second one increasing the luminosity by more than an order of magnitude from nominal, to values above 10^{35} cm^{-2}s^{-1}.

Possible LHC upgrade paths were first examined around 2001 [4]. They have been further developed by the CARE [5] HHH network [6], in collaboration with the US LARP [7].

2 LHC CHALLENGES

Three major challenges faced by the LHC are *collimation and machine protection* [8] including issues such as damage levels, quench thresholds, cleaning efficiency, and impedance; *electron cloud* [9] involving the heat load inside the cold magnets, instabilities, and emittance growth; and *beam-beam interaction* [10], including head-on effects, long-range collisions, weak-strong and strong-strong phenomena. All these effects tend to be more severe for an upgrade.

Another LHC challenge is related to the crossing angle, which, together with the finite bunch length ("hourglass effect"), introduces a geometric luminosity reduction factor [11]

$$R(\phi,\sigma_z,\beta^*) = \frac{1}{\sqrt{\pi}\sigma_z}\int_{-\infty}^{\infty} ds\,\left\{\frac{1}{1+\frac{s^2}{\beta^{*2}}}\right. \exp\left(-\frac{s^2}{\sigma_z^2}\left\{1+\phi^2\frac{1}{1+\frac{s^2}{\beta^{*2}}}\right\}\right)\Bigg\} \quad (1)$$

where β^* designates the IP beta function, σ_z the rms (Gaussian) bunch length, and $\phi \equiv \theta_c\sigma_z/(2\sigma_x^*)$ the so-called "Piwinski angle", with θ_c being the full crossing angle and σ_x^* the rms transverse beam size at the interaction point (IP).

For bunches much shorter than β^* the reduction factor (1) can be approximated as

$$R(\phi,\sigma_z,\beta^*) \approx R(\phi,0,\beta^*) \equiv R(\phi) = \frac{1}{\sqrt{1+\phi^2}} \quad (2)$$

The reduction factor $R(\phi)$ decreases steeply as ϕ is raised beyond nominal, e.g. for smaller β^* and larger crossing angle, as is illustrated in Fig. 1. The nominal LHC operates at $R(\phi) \approx= 0.84$.

If a crab cavity is present, Eq. (1) is modified to

$$R_{\rm cc}(\phi,\sigma_z,\beta^*) = \frac{1}{\sqrt{\pi}\sigma_z}\int_{-\infty}^{\infty}\left\{\frac{1}{1+\frac{s^2}{\beta^{*2}}}\exp\left[-\frac{s^2}{\sigma_z^2}\right.\right. \left.\left.-\frac{\theta_c^2(-k_{\rm cc}s+\sin(k_{\rm cc}s))^2}{4k_{\rm cc}^2\sigma_x^{*2}\left(1+\frac{s^2}{\beta^{*2}}\right)}\right]\right\}, \quad (3)$$

where $k_{\rm cc} \equiv 2\pi/\lambda_{\rm cc}$ denotes the wave number of the crab-cavity rf.

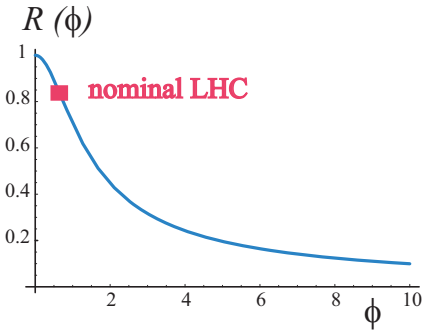

Figure 1: Geometric luminosity reduction factor $R(\phi)$ due to the crossing angle (2), as a function of the Piwinski angle ϕ. The nominal LHC operating point is also indicated.

3 BEAM PARAMETERS

The crossing angle reduces not only the luminosity, but also the beam-beam tune shift, and, thanks to this, for alternating planes of crossing at two interaction points (IPs), the luminosity can be expressed as [11]

$$L \approx \frac{f_{\rm rev}\gamma}{2r_p} n_b \frac{1}{\beta^*} N_b \, \Delta Q_{\rm bb} \, F_{\rm profile} F_{\rm hg} \ , \qquad (4)$$

where $\Delta Q_{\rm bb}$ denotes the total beam-beam tune shift, limited to about 0.01 according to experience at previous hadron colliders, $f_{\rm rev}$ the revolution frequency, N_b the number of protons per bunch, $F_{\rm profile}$ a form factor that depends on the longitudinal profile (about 1 for a Gaussian and $\sqrt{2}$ for a uniform profile) and $F_{\rm hg}$ the reduction factor due to the hourglass effect, which is relevant for bunch lengths comparable to, or smaller than, the IP beta function. In (4) the collision of two round beams has been assumed. Other variables are defined in Table 1, which compares parameters for the nominal and ultimate LHC with those for three upgrade scenarios (abbreviated "ES", "FCC" and "LPA"). The upgrade parameters in (4) which differ from the ultimate LHC configuration are $1/\beta^*$ ($\times 2$), N_b ($\times 2.9$), $\Delta Q_{\rm bb}$ ($\times 1.15$), $F_{\rm profile}$ ($\times\sqrt{2}$) and n_b ($\times 1/2$) for LPA, and $1/\beta^*$ ($\times 6.3$), $\Delta Q_{\rm bb}$ ($\times 1.25$) and $F_{\rm hg}$ ($\times 0.86$) in the ES or FCC schemes, yielding total increases in peak luminosity by factors of 15.5 and 10.6 above nominal, respectively.

Another important consideration for the upgrade is the luminosity lifetime, which can be written

$$\tau_{\rm lum} = \frac{1}{2}\frac{N_b}{\dot{N}_b} = \frac{n_b N_b}{L\sigma} = \frac{4\pi\epsilon\beta^*}{f_{\rm rev} N_b \sigma} \ . \qquad (5)$$

The luminosity lifetime is inversely proportional to the luminosity, or proportional to β^*. The lifetime can be increased only via a higher total beam current, proportional to $n_b N_b$. This implies either more bunches n_b (e.g. a previously considered scheme with 12.5-ns bunch spacing, which was ruled out at the CARE-HHH LUMI'06 workshop in view of excessive heat loads [12]) or a higher charge per bunch N_b, e.g. the LPA scheme. The effective luminosity lifetime can also be increased via "luminosity leveling," namely by suitably varying the beta function, the bunch length, or the crossing angle during a store.

4 EARLY SEPARATION SCHEME

In the **"early-separation" (ES) scenario** [13, 14, 15] one stays with the ultimate LHC beam, squeezes β^* down to about 0.1 m in ATLAS and CMS; and adds early-separation dipoles inside the detectors starting a few metres from the IP. Optionally, ES could also include a quadrupole doublet at about 13 m from the IP [16]. The ES scenario implies installation of new hardware inside the ATLAS and CMS detectors, as well as, most likely, the first ever hadron-beam crab cavities. The latter would gain a factor 2 to 5 in luminosity [15] by ensuring an effective Piwinski angle equal to zero. Their presence is assumed in Table 1. The maximum bunch intensity N_b is linked to the limit on the total beam-beam tune shift for two IPs, via $|\Delta Q_{\rm bb}| = N_b r_p \beta^*/(2\pi\gamma\sigma^{*2}) = N_b r_p/(2\pi(\gamma\epsilon))$, where σ^* denotes the transverse rms beam size at the IP. A maximum beam-beam tune shift of $|\Delta Q_{\rm tot}| = 0.01$ then translates into a maximum bunch population $N_b \approx 1.6 \times 10^{11}$. An IR layout for the ES scheme is sketched in Fig. 2.

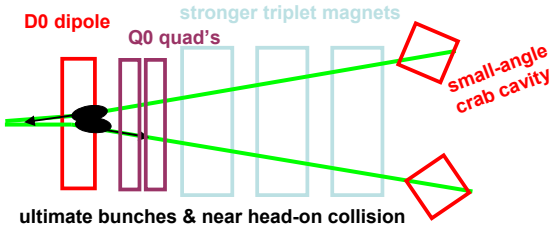

Figure 2: Possible interaction-region layout for the early-separation (ES) scheme, with highly squeezed optics ($\beta^* \approx 0.08$ m).

The merits of the ES scheme are the negligible effect of most long-range collisions thanks to the early separation, the absence of any geometric luminosity loss except for the hourglass effect, and no increase in the beam current beyond ultimate. Challenges include the early separation dipoles 'D0' deep inside the detector, the optional s.c. quadrupole doublet 'Q0', which would also be embedded, strong larger-aperture low-β quadrupoles based on Nb_3Sn, the use of crab cavities for hadron beams [17], the remaining 4 parasitic collisions at 4–5σ separation, a significant off-momentum beta beating (50% at $\delta = 3\times10^{-4}$), which may degrade the collimation efficiency plus low beam and luminosity lifetimes (proportional to β^*). Luminosity leveling via the crossing angle or crab voltage may alleviate this last concern [18].

Table 1: Parameters for the (1) nominal and (2) ultimate LHC compared with those for the three upgrade scenarios with (3) more strongly focused ultimate bunches at 25-ns spacing with either early separation and crab cavities [ES] or full crab crossing [FCC], and (4) longer intense flat bunches at 50-ns spacing in a regime of large Piwinski angle [LPA]. The numbers refer to the performance without luminosity leveling.

parameter	symbol	nominal	ultimate	ES or FCC	LPA
number of bunches	n_b	2808	2808	2808	1404
protons per bunch	N_b [10^{11}]	1.15	1.7	1.7	4.9
bunch spacing	$\Delta t_{\rm sep}$ [ns]	25	25	25	50
average current	I [A]	0.58	0.86	0.86	1.22
normalized transverse emittance	$\gamma\epsilon$ [μm]	3.75	3.75	3.75	3.75
longitudinal profile		Gaussian	Gaussian	Gaussian	uniform
rms bunch length	σ_z [cm]	7.55	7.55	7.55	11.8
beta function at IP1&5	β^* [m]	0.55	0.5	0.08	0.25
(effective) crossing angle	θ_c [μrad]	285	315	0	381
Piwinski angle	ϕ	0.4	0.75	0	2.01
hourglass factor	$F_{\rm hg}$	1.00	1.00	0.86	0.99
peak luminosity	$\hat{L}$ [10^{34} cm^{-2}s^{-1}]	1.0	2.3	15.5	10.6
events per crossing		19	44	294	403
rms length of luminous region	$\sigma_{\rm lum}$ [mm]	45	43	53	37
initial luminosity lifetime	$\tau_{\rm L}$ [h]	22.2	14.3	2.2	4.5
average luminosity ($T_{\rm ta} = 10$ h)	$L_{\rm av}$ [10^{34} cm^{-2}s^{-1}]	0.5	0.9	2.4	2.5
optimum run time ($T_{\rm ta} = 10$ h)	$T_{\rm run}$ [h]	21.2	17.0	6.6	9.5
average luminosity ($T_{\rm ta} = 5$ h)	$L_{\rm av}$ [10^{34} cm^{-2}s^{-1}]	0.6	1.2	3.6	3.5
optimum run time ($T_{\rm ta} = 5$ h)	$T_{\rm run}$ [h]	15.0	12.0	4.6	6.7
e-cloud heat load for $\delta_{\rm max} = 1.4$	$P_{\rm ec}$ [W/m]	1.07	1.04	1.0	0.4
e-cloud heat load for $\delta_{\rm max} = 1.3$	$P_{\rm ec}$ [W/m]	0.44	0.6	0.6	0.1
SR heat load	$P_{\rm SR}$ [W/m]	0.17	0.25	0.25	0.36
image-current heat load	$P_{\rm ic}$ [W/m]	0.15	0.33	0.33	0.70

Complementary Crab Cavities

In the ES scheme the geometric luminosity loss for a large crossing angle can be reduced either by bunch shortening rf or by crab cavity rf. It is instructive to compare the voltage required for the two cases [19].

The voltage required for bunch shortening is

$$V_{\rm rf} \approx \left[\frac{\epsilon_{||,\rm rms}^2 c^3 C\eta}{E_0 e\pi f_{\rm rf}}\right] \frac{1}{\sigma_z^4} \approx \left[\frac{\epsilon_{||,\rm rms}^2 c^3 C\eta}{E_0 e\pi f_{\rm rf}}\right] \frac{\theta_c^4}{\phi^4\, 16\, {\sigma_x^*}^4}\ . \tag{6}$$

Equation (6) reveals an unfavorable scaling of the rf voltage with the 4th power of the crossing angle and the inverse 4th power of the IP beam size. The voltage can be decreased, to some extent, by reducing the longitudinal emittance (but limits come from intrabeam scattering, loss of Landau damping, and the injectors) and by increasing the rf frequency (the voltage scales inversely with the rf frequency).

By contrast, assuming horizontal crossing, the crab cavity voltage required is

$$V_{\rm cc} = \frac{cE_0 \tan(\theta_c/2)}{e2\pi f_{\rm rf,cc} R_{12}} \approx \frac{cE_0}{e4\pi f_{\rm rf} R_{12}}\,\theta_c\ . \tag{7}$$

It is linearly proportional to the crossing angle and independent of the IP beam size. The voltage scales with $1/R_{12}$, where R_{12} is the (1,2) transport matrix element from the location of the crab cavity to the IP. As in the case of the bunch shortening rf, the crab-cavity voltage is also inversely proportional to the crab-rf frequency.

Figure 3 illustrates the voltages required for bunch shortening and for crab cavities, respectively, as a function of the crossing angle. The attractivity of crab cavities is evident. Figure 4 highlights the luminosity gain from a crab cavity for the ES and FCC schemes with an IP beta function β^* of 0.11 m. The residual $\sim$15% luminosity reduction at zero crossing angle is due to the hourglass effect, as β^* is comparable to the bunch length.

5 FULL CRAB CROSSING SCHEME

Crab cavities with sufficiently large total voltage could provide the same luminosity, and would allow for identical beam parameters, as the early separation (ES)) scheme, while avoiding the need for accelerator magnets inside the detectors. Possible beam parameters for such **"full crab crossing" (FCC) scenario** are identical to those of the ES scheme, as is indicated in Table 1. A corresponding IR layout is sketched in Fig. 5.

In the FCC scheme the crossing angle could be raised to any value supported by the triplet aperture and the crab-

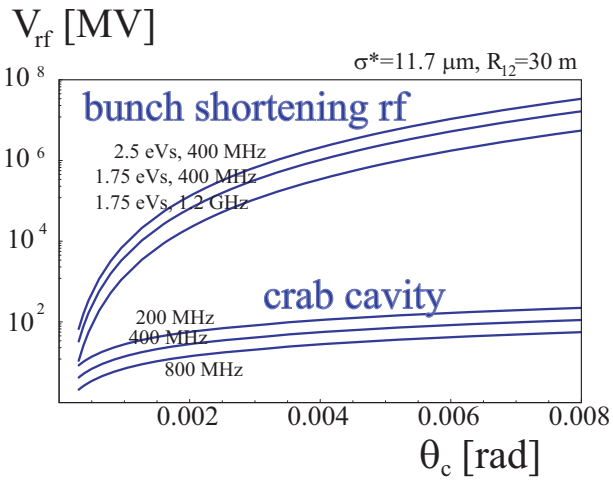

Figure 3: Bunch shortening rf voltage required to maintain a constant value $R(\phi) = 0.68$ and crab-cavity voltage as a function of the full crossing angle, for different rf frequencies and longitudinal emittances. The curves are computed from Eqs. (6) and (7). An IP beam size of 11.7 μm and $R_{12} = 30$ m from the crab cavity to the IP are assumed [19].

cavity system. For example, a transverse beam-beam separation of 8σ at the parasitic collisions is likely to be sufficient for avoiding performance degradation due to long-range beam-beam effects, provided a long-range wire compensation is also put in place.

The merits of the FCC scheme are the absence of any geometric luminosity loss except for the hourglass effect, no parasitic collisions at reduced separation, the absence of accelerator elements inside the detector, and no increase in the beam current beyond ultimate. A few of the ES challenges remain for FCC, namely the required strong larger-aperture low-β quadrupoles based on Nb_3Sn, the use of crab cavities for hadron beams (with 60% higher crab voltage than for ES), a significant off-momentum beta beating (50% at $\delta = 3 \times 10^{-4}$), plus low beam and luminosity lifetimes. Luminosity leveling via the crab voltage would be an option.

As an illustration, we consider an IP beta function $\beta^* = 0.08$ m, a crab cavity operating at 400 MHz and a typical (1,2) transport matrix element $R_{12} \approx 30$ m between the crab cavity and the IP. In this case the crossing angle needed for ES would be about 0.4 mrad (with 5σ separation), compared with 0.64 mrad for FCC (8σ separation). Using (7) these numbers translate into local crab-cavity voltages of 5.6 MV for ES and 9.0 MV for FCC. In other words, a 60% increase in the total crab voltage would be equivalent to the early-separation dipole.

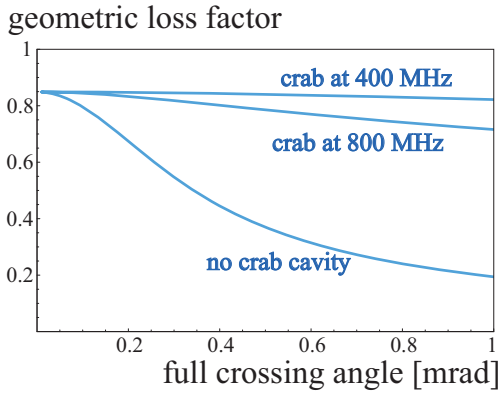

Figure 4: Luminosity reduction factor as a function of crossing angle without a crab cavity, and with a crab cavity operated at 400 MHz and 800 MHz, respectively, assuming $\beta^* = 0.11$ m. A crossing angle of 5 times the rms divergence (5 σ separation at the closest long-range encounters) would be 0.34 mrad, while 8σ separation at the closest parasitic encounters would translate to a 0.54-mrad crossing angle.

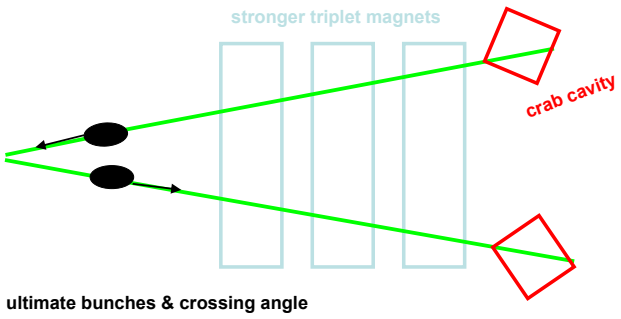

Figure 5: Possible interaction-region layout for the full crab-crossing (FCC) scheme, with highly squeezed optics ($\beta^* \approx 0.08$ m).

6 LARGE PIWINSKI ANGLE SCHEME

In the **"large Piwinski angle" (LPA) scenario** the bunch spacing is doubled, to 50 ns; longer, longitudinally flat, and more intense bunches are collided with a large Piwinski angle of $\phi \equiv \theta_c \sigma_z / (2\sigma^*) \approx 2$; the IP beta function is reduced by a more moderate factor of 2 to $\beta^* \approx 0.25$ m; and long-range beam-beam wire compensators [20] are installed upstream of the inner triplets. This regime of large ϕ and uniform bunch profile allows raising the bunch intensity N_b in (4) and thereby the luminosity, since lengthening the bunches in proportion to N_b maintains a constant value of $\Delta Q_{\rm bb}$. Figure 6 illustrates the IR layout for this upgrade option.

The merits of the LPA scheme are the absence of accelerator elements inside the detector, no crab cavities, reduced IR chromaticity, and relaxed IR quadrupoles. For

$\beta^* \approx 0.25$ m various possible optics solutions based on large-aperture NbTi quadrupoles exist [21], though the survival of the latter at high luminosity still remains to be demonstrated. Challenges are the operation with large Piwinski angle, unproven for hadron beams, the high bunch charge, in particular the beam production and acceleration through the SPS, the larger beam current, the (almost established) wire compensation, and an off-momentum beta beating of about 30% at $\delta = 3 \times 10^{-4}$. The level of off-momentum beta beating is about half that of the ES scheme, but approximately two times larger than for the nominal LHC, and likely to impact the collimation cleaning efficiency.

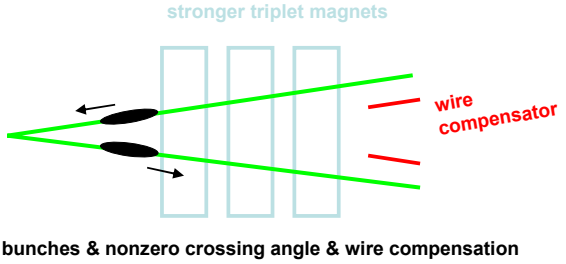

Figure 6: Interaction-region layout for large-Piwinski-angle (LPA) upgrade with an IP beta function of 0.25 m.

FLAT BUNCHES AND LARGE ϕ

The merits of longitudinally "flat" bunches and a large Piwinski angle can be unveiled more clearly by rewriting the luminosity expression in terms of the maximum beam-beam tune shift (which is taken to be the same and constant) for bunches with both Gaussian and uniform profiles.

As before and as appropriate for the LHC upgrade, we consider two interaction points (IPs) with alternating crossing. If the crossing angle is small, $\theta_c \ll 1$, the transverse IP beam size smaller than the bunch length, and the latter smaller than the IP beta function, $\sigma^* \ll \sigma_z \ll \beta^*$, and if furthermore the Piwinski angle is larger than 1, $\phi \gg 1$, the luminosity for bunches with Gaussian longitudinal profile can approximately be written [22]

$$L_{\rm gauss} \approx \frac{1}{2}\frac{f_{\rm rev} n_b \gamma}{r_p \beta^*} \Delta Q_{\rm bb} N_b \ , \qquad (8)$$

where $\Delta Q_{\rm bb}$ denotes the total linear beam-beam tune shift from the two interaction points, experienced at the center of the bunch.

Also for our second case of longitudinally "flat" bunches we assume a reasonably small crossing angle, $\theta_c \ll 1$. If in addition, the crossing angle is larger than the rms beam divergence, $\theta_c \gg \sqrt{\epsilon_N/(\gamma\beta^*)}$ (a logical requirement if the crossing angle is meant to separate the beams at the next parasitic encounter), and if the total bunch length l_b is larger than the effective extent of the beam intersection, $l_b \gg \sigma^*/\theta_c$, we can re-express the luminosity for bunches with flat longitudinal profile as [22]

$$L_{\rm flat} \approx \frac{1}{\sqrt{2}}\frac{f_{\rm rev} n_b \gamma}{r_p \beta^*} \Delta Q_{\rm bb} N_b \ . \qquad (9)$$

Comparison of (8) and (9) shows that, for the same number of particles per bunch N_b, and the same total tune shift from two IPs $\Delta Q_{\rm bb}$, the luminosity will be $\sqrt{2} \approx 1.4$ times higher with a "flat" distribution. The above assumptions were implicitly made when we earlier quoted the value of the form factor $F_{\rm profile}$ in (4).

As an additional merit, it is only in the regime of large Piwinski angle and for flat bunches that the number of particles N_b can be increased independently of the total tune shift $\Delta Q_{\rm bb}$, by lengthening the bunches.

7 CRAB WAIST COLLISIONS

All upgrade scenarios, LPA, ES and FCC, could conceivably be adapted for crab-waist collisions [23] by operating with flat beams with $\beta_x^* \gg \beta_y^*$, which would also make optimum use of the available aperture in the low-beta quadrupoles [24], and preferably with higher intensity and higher brightness. In addition, crab-waist collisions require a large Piwinski angle, such as the one for the LPA scheme, a small beta function comparable to σ_x^*/θ_c such as as for the ES or FCC scheme, and crab-waist sextupoles [25].

A possible approach for implementing crab-waist collisions at the LHC, therefore, is to adopt flat beams, combine some key ingredients of the ES, FCC and LPA schemes, and add suitable sextupoles in the IRs.

8 LUMINOSITY EVOLUTION

Figure 7 compares the luminosity evolution for the three scenarios. A turn-around time (the time between the end of a collision run and the start of the next collisions) of 5 h and the corresponding optimum run durations from Table 1 are assumed. The dashed lines indicate the respective time-averaged luminosities.

Without leveling the instantaneous luminosity decays as

$$L(t) = \frac{\hat{L}}{(1 + t/\tau_{\rm eff})^2} \ , \qquad (10)$$

with

$$\tau_{\rm eff} \equiv \frac{n_b N_b(0)}{\hat{L}\sigma_{\rm tot} n_{IP}} \qquad (11)$$

denoting the effective beam lifetime due to burn-off at the collision points, $\sigma_{\rm tot} \approx 100$ mb the relevant total cross section, n_{IP} the number of IPs, and $\hat{L}$ the initial peak luminosity. The optimum average luminosity is

$$L_{\rm av} = \frac{\hat{L}\tau_{\rm eff}}{(\tau_{\rm eff}^{1/2} + T_{\rm ta}^{1/2})^2} \ , \qquad (12)$$

where T_{ta} denotes the turn-around time. The optimum run time $T_{\rm run}$ is the geometric mean of effective lifetime and

turn-around time:

$$T_{\rm run} = \sqrt{\tau_{\rm eff} T_{\rm ta}}\,. \qquad (13)$$

In Fig. 7 it can be seen that the luminosity for the ES or FCC scenarios starts higher, but decays faster than for the LPA case, leading to shorter runs. The average luminosity values are nearly identical. The high initial peak luminosity for ES or FCC may not be useful for physics in view of possibly required set-up and tuning periods. On the other hand, the average event pile up for the ES and FCC options is about 30–40% lower than that for the LPA case, since there are twice as many bunches and collisions.

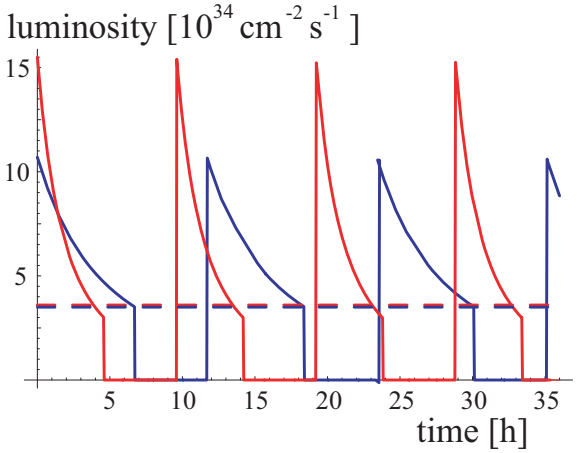

Figure 7: Ideal luminosity evolution without leveling for the ES or FCC (red) and LPA scenarios (blue), assuming the optimum run duration for a turn-around time of 5 h. The dashed lines indicate the corresponding time-averaged luminosities.

Smaller pile up at the start of a physics run, and higher luminosity at the end of each run would be desirable. Such luminosity leveling could be accomplished by dynamic β^* squeeze, crossing angle variation [18] for ES, or changes in the crab rf voltage for ES or FCC, and equally by dynamic β^* squeeze or via bunch-length reduction for LPA.

Leveling provides a constant luminosity, equal to L_0, and the beam intensity then decreases linearly with time t as

$$N_b = N_{b0} - \frac{L_0 \sigma_{\rm tot} n_{IP}}{n_b} t\,. \qquad (14)$$

The accessible intensity range $\Delta N_{b,\rm max}$ is limited, for example, by the range of the leveling variable, e.g. by the minimum value of β^*, so that the length of a run amounts to

$$T_{\rm run} = \frac{\Delta N_{b,\rm max} n_b}{L_0 \sigma_{\rm tot} n_{IP}}\,, \qquad (15)$$

and the average luminosity with leveling becomes

$$L_{\rm av,lev} = \frac{L_0}{1 + \Delta N_{b,\rm max} n_b T_{ta} / \left(L_0 \sigma_{\rm tot} n_{IP}\right)}\,. \qquad (16)$$

Table 2: Event rate, run time, and average luminosity for the three upgrade scenarios with leveling. Highlighted in bold are two promising examples.

	ES or FCC	LPA
events/crossing	300	300
optimum run time	N/A	2.5 h
av. luminosity [10^{34} cm^{-2}s^{-1}]	N/A	2.6
events/crossing	150	150
optimum run time	2.5 h	**14.8 h**
av. luminosity [10^{34} cm^{-2}s^{-1}]	2.6	2.9
events/crossing	75	75
optimum run time	**9.9 h**	26.4 h
av. luminosity [10^{34} cm^{-2}s^{-1}]	2.6	1.7

Table 2 compares event rates, run times, and average luminosity values achievable in the ES or FCC and LPA schemes. In case of β^* variation, the tune shift decreases during the store, while for leveling via the bunch length or crossing angle the tune shift increases. With leveling, the sensitivity of the average luminosity to the accessible range of the leveling parameter (β^*, bunch length or crossing angle) greatly depends on the chosen number of events per crossing, as is illustrated in Fig. 8.

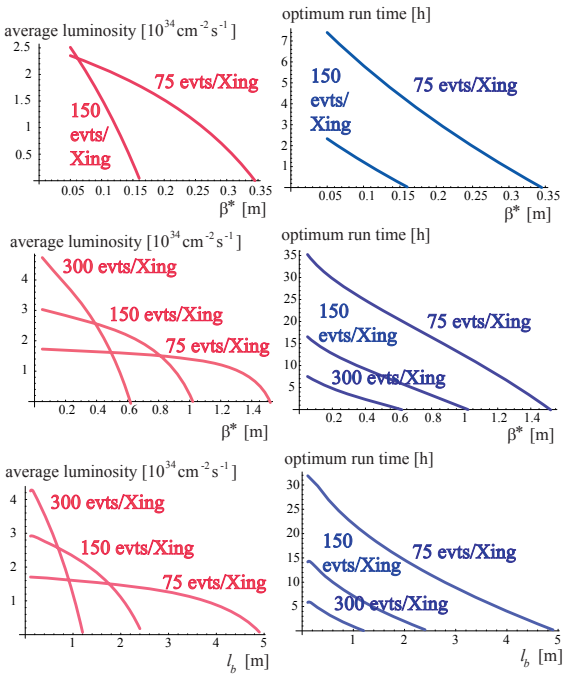

Figure 8: Average luminosity (left) and optimum run time (right) as a function of final β^* for ES or FCC with β^* leveling (top) and for LPA with β^* leveling (center), and as a function of l_b [total bunch length] for LPA with l_b leveling (bottom).

9 LUMINOSITY REACH

Figure 9 illustrates the dependence of the geometric luminosity reduction on the IP beta function. The two lower curves refer to a crossing angle of 9.5 or 5 times the rms IP beam divergence, respectively. The top curve represents both the early separation scheme with complementary crab cavity and also the full crab crossing scheme. The crab cavity restores most of the geometric overlap, except at very small β^* values, where the hourglass reduction becomes significant.

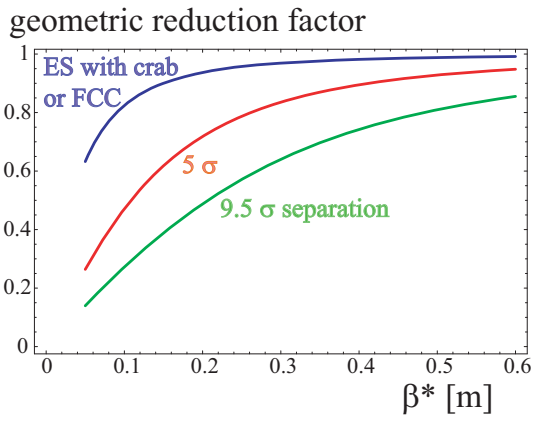

Figure 9: Geometric luminosity reduction as a function of β^* with 9.5σ (nominal) and 5σ separation (ES scheme without crab cavity) at the closest long-range encounters, as well as for arbitrary separation including crab crossing (ES with crab cavity or FCC).

Figure 10 shows the average luminosity as a function of β^* for four scenarios: the large-Piwinski angle (LPA) scheme, the early-separation (ES) scheme with either 9.5σ or 5σ beam-beam distance at the nearest long-range encounters if no crab cavity is employed, as well as ES with crab cavity or full crab crossing (FCC). The average luminosity shown is the ideal value (12), with an assumed turnaround time of 5 hours that could be provided by an upgraded LHC injector complex. For comparison, the average luminosities and β^* values corresponding to the nominal and the "ultimate" LHC with 10-h turnaround time are also indicated by plotting symbols.

The figure demonstrates that the performance of the ES scheme is considerably boosted by a crab cavity, but that both ES with crab cavity and FCC require β^* values below about 0.1 m in order to achieve the same average luminosity as obtained for the LPA scheme with a relaxed beta function of $\beta^* \approx 0.25$ m.

The LPA parameters in this example were chosen so that $|\Delta Q_{\rm tot}| \approx 0.011$ at $\beta^* \approx 0.25$ m. The magnitude of the LPA tune shift decreases if β^* is squeezed towards smaller values, a feature which could be exploited to further raise the integrated LPA luminosities for $\beta^* < 0.25$, e.g. by shortening the bunches. On the other hand, for constant normalized separation and constant bunch length, the total tune shift grows with increasing β^*, which may reduce the average LPA luminosity achievable for $\beta^* > 0.25$ m.

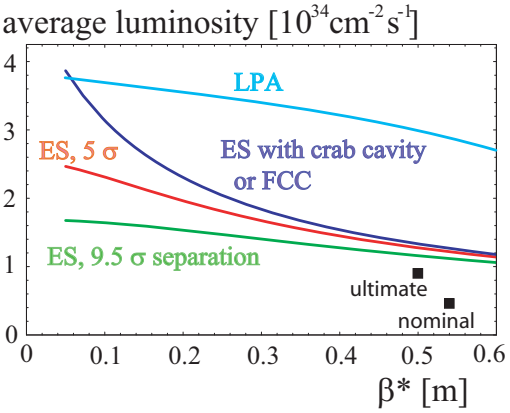

Figure 10: Average luminosity as a function of β^* for the large-Piwinski angle (LPA) scheme with a constant normalized separation of 8.5σ and a constant bunch length; for the early separation (ES) scheme with constant 9.5σ or 5σ separation and no crab cavity; and for ES with crab cavity or full crab crossing (FCC).

10 LHCB COMPATIBILITY

An upgrade of LHCb to Super-LHCb is planned, in order to exploit luminosities up to 2×10^{33} cm^{-2}s^{-1}, or 2% of the luminosity delivered to ATLAS and CMS. The LHCb detector is special due to its asymmetric location in the ring, which opens up a new possibility of supplying LHCb with its target possibility.

In the LPA case with 50-ns spacing between successive bunches in a train, we can arrange to have either collisions between the 50-ns bunches or no collisions at all in LHCb [27], depending on the distance in multiples of 25 ns which we choose between the various groups of bunch trains distributed around the ring. At 50-ns spacing, satellite bunches can be added in between the main bunches, as is illustrated in the bottom part of Fig. 11, displaying possible bunch patterns for various LHC configurations. Such satellites may be produced by asymmetric bunch splitting in the PS (possibly large fluctuation). In LHCb these satellites can be made to collide with main bunches at 25-ns time intervals. The intensity of the satellites should be lower than about 3×10^{10} protons per bunch in order to add less than 5% to the total tune shift and also to avoid electron-cloud problems. A beta function of about 3 m would result in the desired luminosity equivalent to 2×10^{33} cm^{2}s^{-1}. This value of β^* is easily possible with the present LHCb IR magnets and layout, which allows β^* squeezes down to 2 m [28].

For the ES or FCC scenarios with 25-ns bunch spacing, as well as for a different LPA filling with main-bunch collisions at LHCb, the resulting head-on collisions at Super-LHCb would contribute to the beam-beam tune shift of the

bunches colliding in ATLAS and CMS, which would lower the peak luminosity for the latter. Two ways out are (1) colliding only during the second half of each store when the beam-beam tune shifts from IP1 and 5 have sufficiently decreased below the beam-beam limit, or (2) introducing a transverse collision offset, albeit the latter raises concerns about offset stability, interference with collimation, poor beam lifetime, background etc. Requiring an LHCb contribution to the total tune shift of less than 10% implies transverse beam-beam offsets larger than 4.5σ, and $\beta^* \approx 0.08$ m, which is incompatible with the present LHCb IR configuration. For either option, the average luminosity delivered to Super-LHCb is considerably lower than for the LPA case with satellites.

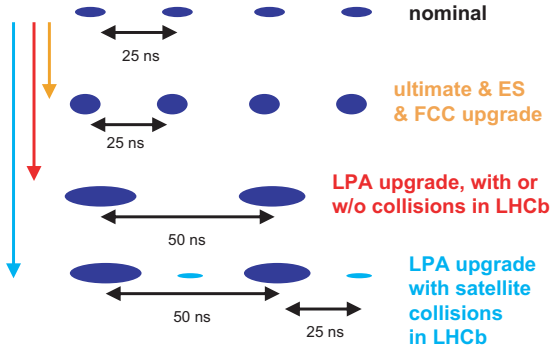

Figure 11: Bunch structures for nominal LHC, ultimate, ES or FCC upgrade, LPA upgrade, and LPA with satellite-bunch collisions at LHCb.

11 INJECTOR UPGRADE

An LHC injector upgrade is the central component of the CERN DG's White Papers [26]. The injector upgrade is already needed to produce the ultimate LHC beam (1.7×10^{11} protons per bunch with nominal beam emittance). In the context of the LHC upgrade, it will also provide a reduced turnaround time and, thereby, a higher integrated luminosity.

In order to provide the needed beam quality and intensity the existing 50-MeV proton Linac2 will be replaced by a 160-MeV "Linac4", and in the longer-term future extended by a 5-GeV s.c. proton linac (SPL). This will not only render the 1.4-GeV PS booster obsolete, but in addition it will raise the injection energy of the following storage ring PS2. The PS2 is a proposed successor of the present PS with twice the circumference and about twice the top energy (50 GeV). The next and last machine in the LHC injector chain is the Super Proton Synchrotron (SPS), which, though remaining, will be enhanced to cope with stronger electron-cloud effects and higher beam intensity.

The upgraded injector complex is designed to deliver to the LHC a beam with a maximum bunch intensity of 4×10^{11} at 25-ns bunch spacing. With this injector, the beam production for the ES scheme is straightforward. The LPA beam, requiring a slightly higher bunch population of 5×10^{11} at 50-ns bunch spacing, might be obtained by omitting the last double splitting in the PS, or in the future PS2 if the PS2 beam is still manipulated in a similar fashion as the present SPS. Numerous techniques for bunch flattening are at hand [29].

In the much longer term the SPS could be replaced by a higher-energy s.c. machine that would feed a higher-energy version of the LHC. R&D for an LHC energy upgrade is discussed in Refs. [30, 31], while the conceptual design for an energy tripler magnet can be found in [32].

12 CONCLUSIONS

We have presented three scenarios of the LHC luminosity upgrade, all promising a peak luminosity in excess of 10^{35} cm^{-2}s^{-1} with acceptable heat load and pile-up rate. Luminosity leveling should be seriously considered for the increased pile-up rates of the upgraded LHC, as it would provide a more regular flow of events at the possible expense of a moderate decrease in average luminosity.

The early separation (ES) and full crab-crossing (FCC) schemes both push β^*. ES requires slim magnets inside the detector, crab cavities, and Nb_3Sn quadrupoles. Also a "Q0" doublet inside the detector could optionally be added to achieve minimum β^* values. FCC requires 60% stronger crab cavities and wire compensation of residual long-range beam-beam effect. The ES and FCC schemes are particularly attractive if the total beam current in the LHC is limited. Luminosity leveling for ES and FCC can be realized by varying β^*, θ_c or the crab voltage. An open issue for ES is the effect of a few long-range collisions with reduced separation, which is avoided for FCC.

The large Piwinski angle (LPA) scheme entails fewer bunches of higher charge and an only moderately decreased β^*. It can conceivably be realized with NbTi magnet technology if necessary. The "Q0" doublet may also be an option for this scenario. LPA is more flexible in regard to collisions at LHCb. The LPA luminosity can be leveled by varying the bunch length or β^*. Open issues for LPA are the beam production, transport and acceleration through the SPS, and also hadron beam-beam effects at large Piwinski angle.

The off-energy beta beating compromises the collimation cleaning efficiency. This is a common concern for the three scenarios, but more severe for the lower β^* value of ES or FCC. The crab-waist scheme is yet another promising upgrade path that should further be explored for the LHC.

The first two or three years of LHC operation will clarify the severity of the electron cloud, long-range beam-beam collisions, collimator impedance, etc. On the same time scale, the first LHC physics results will indicate whether or not magnetic elements can be installed inside the detectors. Also around 2011, the LHC crab-cavity R&D, which — motivated by CARE-HHH discussions — is now being set up in a broad international collaboration, will have reached

a conclusion on the feasibility of LHC crab cavities and a solid cost estimate. The outcome from all these activities will finally decide the choice of the upgrade path.

13 ACKNOWLEDGEMENT

Many colleagues contributed to the ideas presented in this paper.

14 REFERENCES

[1] A. de Roeck, "Physics at the Next Colliders," Third National Turkish Accelerator Congress (UPHUK3), Bodrum, Turkey, 2007.

[2] J. Strait, private communication (2003).

[3] Physics Potential and Experimental Challenges of the LHC Luminosity Upgrade, F. Gianotti, M.L. Mangano, T. Virdee (conveners), CERN-TH/2002-078 (2002).

[4] O. Brüning et al, "LHC Luminosity and Energy Upgrade: A Feasibility Study," LHC-PROJECT-Report-626 (2002).

[5] *http://esgard.lal.in2p3.fr/Project/Activities/Current*

[6] *http://care-hhh.web.cern.ch/CARE-HHH*

[7] *http://www.agsrhichome.bnl.gov/LARP*

[8] *http://lhc-collimation-project.web.cern.c/lhc-collimation-project*

[9] *http://ab-abp-rlc.web.cern.ch/ab-abp-rlc-ecloud*

[10] *http://lhc-beam-beam.web.cern.ch/lhc-beam-beam*

[11] F. Ruggiero, F. Zimmermann, "Luminosity Optimization Near the Beam-Beam Limit by Increasing Bunch Length or Crossing Angle," PRST-AB 5, 061001 (2002).

[12] L. Tavian, "Cryogenic Limits," CARE-HHH LUMI'06 workshop, Valencia, 16–20 October 2006; *http://care-hhh.web.cern.ch/CARE-HHH/LUMI-06/*; and W. Scandale, F. Zimmermann, "IR Ranking Proposal and New Beam Parameter Sets for the LHC Upgrade — The View of HHH," Proc. CARE-HHH LUMI'06, Valencia, CERN Yellow Report CERN-2007-002, p. 99 (2006)

[13] J.-P. Koutchouk, "Possible Quadrupole-First Options with $\beta^* \leq 0.25$ m," Proc. CARE-HHH LHC-LUMI-05, Arcidosso, CERN Yellow Report CERN-2006-008, p. 41 (2006)

[14] J.-P. Koutchouk, "Strong Focusing Insertion Solutions for the LHC Luminosity Upgrade," Proc. CARE-HHH LHC-LUMI-06, Valencia, CERN Yellow Report CERN-2007-002, p. 43 (2007)

[15] E. Todesco, R.W. Assmann, J.-P. Koutchouk, E. Metral, G. Sterbini, F. Zimmermann, R. De Maria, "A Concept for the LHC Luminosity Upgrade Based on Strong Beta* Reduction Combined with a Minimized Geomtrical Luminosity Loss Factor," PAC'07, Albuquerque (2007).

[16] E. Laface et al, private communication; see also E. Laface, "Q0 Status," CARE-HHH IR07 workshop, Frascati, 6-8.11.2007, *http://care-hhh.web.cern.ch/CARE-HHH/IR07*

[17] R. Calaga, K. Akai, K. Ohmi, K. Oide, U. Dorda, R. Tomas, F. Zimmermann, "Small Angle Crab Compensation for LHC IR Upgrade," PAC'07, Albuquerque (2007).

[18] G. Sterbini, J.-P. Koutchouk, "A Luminosity Leveling Method for LHC Luminosity Upgrade Using an Early Separation Scheme," LHC-Project-Note-403 (2007).

[19] F. Zimmermann, U. Dorda, "Progress of Beam-Beam Compensation Schemes," Proc. CARE-HHH-APD Workshop LUMI'05, Arcidosso, CERN Yellow Report CERN-2006-008, p. 55 (2005).

[20] U. Dorda, W. Fischer, V.D. Shiltsev, F. Zimmermann, "LHC Beam-Beam Compensation Using Wires and Electron Lenses," PAC'07, Albuquerque (2007).

[21] O. Brüning, R. De Maria, R. Ostojic, "Low Gradient, Large Aperture IR Upgrade Options for the LHC Compatible with Nb-Ti Magnet Technology," LHC-PROJECT-Report-1008 (2007).

[22] F. Ruggiero, G. Rumolo, F. Zimmermann, Y. Papaphilippou, "Beam Dynamics Studies for Uniform (Hollow) Bunches or Super-Bunches in the LHC: Beam-Beam Effects, Electron Cloud, Longitudinal Dynamics, and Intrabeam Scattering," Proc. RPIA2002, Tsukuba, Japan, CERN-LHC-Project-Report-627 and KEK Proceedings 2002-30 (2002)

[23] P. Raimondi, "New Developments in Super B Factories," Proc. PAC'07, Albuquerque (2007).

[24] S. Fartoukh, "Flat Beam Optics," LHC MAC, 16.06.2006 *http://cern.ch/mgt-lhcmac*

[25] P. Raimondi, M. Zobov, D. Shatilov, "Beam-Beam Simulations for Particle Factories with Crabbed Waist," Proc. PAC'07, Albuquerque (2007).

[26] CERN DG White Papers, June 2006.

[27] M. Ferro-Luzzi, private communication, January 2008.

[28] W. Herr, Y. Papahilippou, "Alternative Running Scenarios for the LHCb Experiment," LHC-Project-Report-2009 (2007).

[29] F. Zimmermann, "Generation and Stability of Intense Long Flat Bunches," CARE-HHH BEAM'07, CERN, 1-5 October 2007, *http://care-hhh.web.cern.ch/CARE-HHH/IR07*, these proceedings (2008).

[30] LBNL S.c. Magnet Program Newsletter, no. 2 "HD-1 Sets New Dipole Field Record" (2003).

[31] *http://lt.tnw.utwente.nl/project.php?projectid=9*

[32] P. McIntyre et al, "On the Feasibility of a Tripler Upgrade for LHC," PAC'05, Knoxville (2005).